

# Detectability of the Image Operation Order: Upsampling and Mean Filtering

Jiana Li\*, Xin Liao\*<sup>†</sup>, Rongbing Hu\* and Xuchong Liu\*<sup>†</sup>

\*College of Computer Science and Electronic Engineering

Hunan University, Changsha, China

<sup>†</sup>Key Laboratory of Network Crime Investigation of

Hunan Provincial Colleges, Changsha, China

<sup>‡</sup>Corresponding author: xinliao@hnu.edu.cn

**Abstract**—As image modification and tampering, especially multiple editing operations, prevail in today’s world, identifying authenticity and credibility of digital images becomes increasingly important. Recently, two editing operations, upsampling and mean filtering, have attracted increasing attention. While there are many existing image forensics techniques to identify the existence and order of specific operations in a certain processing chain, few detecting methods are concerned about the order of upsampling and mean filtering operations. Following some strongly indicative analysis in different domains of DFTs of images’ p-maps, this paper discusses a newly designed method which utilizes features to determine the order of upsampling and mean filtering operations. Specifically, our goal is to use two features, the symmetry-based PSNR and the fourth order energy fitting curve, to characterize the features of operation chains in the DFTs of images’ p-maps. We calculate the variance of the fitting curve and examine the change of fingerprints under different operating intensities to ensure these two features can be broadly applied to operation detection. These features are fed to SVM, effectively discriminating among five combinations of upsampling and mean filtering. The representative experiments can verify the effectiveness of the proposed method.

**Index Terms**—Image forensics, Operation chain detection, Upsampling, Mean filtering, Symmetry-based PSNR, Fourth order energy fitting curve.

## I. INTRODUCTION

Nowadays, powerful multimedia editing tools lower the cost of manipulating images and allow unskilled users to modify their images much easier. It becomes increasingly difficult to determine whether or not an image content is authentic, and this undermines the life, reputation, social fairness and so on. Therefore, it is crucial to detect the primitiveness, authenticity, integrity of images in order to prevent malicious image tampering [1].

Digital image forensics has been developed rapidly to solve these problems [2]. With the development of forensic methods, the detection technologies for single operations are relatively mature. For example, Farid et al. [3] investigated an expectation/maximization algorithm for resampling detection and used the consistency of light source projection to detect the authenticity of an image [4]. Fridrich team presented a method for detecting copy-move forgery [5]. There are many other detecting approaches for exposing image splicing [6,7], the compression [8-10], median filtering [11,12], contrast enhancement [13,14] and blurring [15,16].

A significant drawback of the above forensic techniques is that they are designed to detect a single operation. Unfortunately, in real scenarios, their application is limited. Since it is likely to apply multiple processing operators, and each operation alters the fingerprints exploited by current forensic tools. At this point, there is an urgent need to develop technology for multiple-operations order detection. The operation chain that involves JPEG compression and resampling was studied in [17] to understand whether the image has undergone a single JPEG compression or followed by resampling. Gao et al. [18] extracted impulsive gaps and zeros left in the histogram to discriminate the operation chain: contrast enhancement and resizing. Recently, in refs. [19,20], Chu et al. designed a new multiple-hypotheses framework which aims at detecting the order of resizing and blurring operations and determining the condition of when we can distinguish all considered orders.

This paper focuses on the order detection of upsampling and mean filtering. Upsampling is commonly used for enlarging images in order to display on a higher resolution application, while mean filtering makes image denoise and smooth. Imagine an image life, in which a digital image was upsampled for the web, calibration, business after being captured by a digital camera. Then, it might be mean filtered for eliminating image noise caused by upsampling. Thus, given a suspicious image, it is important to understand whether the image has undergone upsampling and mean filtering. Despite a great variety of existing forensic methods, such as resampling detection scheme [3,21], little attention has been paid to the case where involve upsampling and mean filtering operation. As a result, the upsampling and mean filtering order detection becomes an unresolved forensic issue in the recovery of the processing order of an image.

In this paper, we propose a new method to detect the order of upsampling and mean filtering operations. Our main work can be divided into two parts: the feature extraction method and detectability analysis. The feature extraction method is based on p-maps, detecting upsampling and mean filtering operation chains. P-map [4] is a probability matrix with each element representing the probability of the corresponding image pixel correlated with its neighbor pixels. Two proposed features defined from the discrete Fourier transform (DFT) of images’ p-map are named symmetry-based peak signal

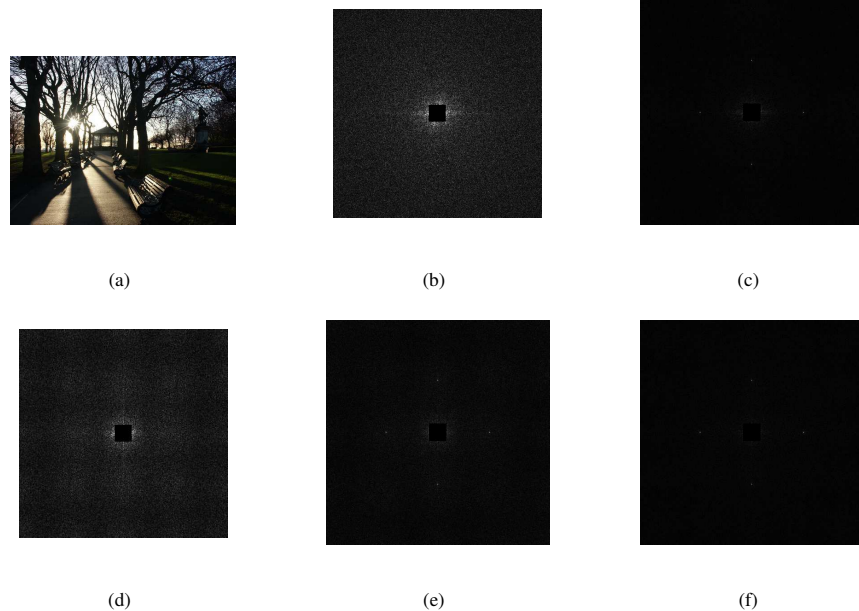


Fig. 1. Fingerprints for operation detecting. (a) is the original image. (b) - (f) show the DFTs of the p-map of images. The operations of images are (b) unaltered, (c) scaling, (d) mean filtering, (e) scaling and then mean filtering, and (f) mean filtering and then scaling. Take the zoom factor of 1.3 and the filter window size of 4 as an example.

to noise ratio (PSNR) and fourth order energy fitting curve. The symmetry-based PSNR simplifies the process of detecting upsampling operations by the symmetry of the probability spectrum. Then, we calculate the variance of the energy fitting curve to characterize errors between the energy fitting curve and the actual energy curve. Moreover, the detectability of the order of operations with different intensities is analyzed to ensure these two features are useful in detecting operations. These features are then input to SVM that explores the hidden information about the order of upsampling and mean filtering operations, excellently distinguishing the order of operation chains in each image. A public image library is examined to demonstrate the effectiveness of our proposed method. Experimental results show that the average classification accuracy of the proposed method is above 90%.

The remaining of this paper is organized as follows. In the Section II, we extract symmetry-based PSNR and the fourth order energy fitting curve to characterize operation chains. The detectability analysis of the order of operations under different intensities of operations is shown in Section III. To validate the effectiveness of our proposed method, Section IV presents experimental results on the image library. Finally, Section V summarizes the main conclusion of this work.

## II. THE FEATURE EXTRACTION OF UPSAMPLING AND MEAN FILTERING OPERATIONS

To estimate the processing history of multiple operations, it is necessary to detect the existence of each operation and the order of the chain of operations. Therefore, we consider the following five hypotheses for the history of a given image.

$H_1$ : The image is unaltered.

H<sub>2</sub>: The image is only altered by upsampling.

$H_3$ : The image is only altered by mean filtering.

$H_4$ : The image is altered by upsampling then mean filtering.  
 $H_5$ : The image is altered by mean filtering then upsampling.

In order to distinguish these hypotheses, we need to find out their differences. In the following subsection A, after analyzing a great number of images with different hypotheses and intensities of operation, it can be observed that each hypothesis has its unique fingerprints in the DFT of an image's  $\phi$ -map. Depending on the fingerprints derived in subsection A, we present two features to discriminate these hypotheses. The features are proposed in subsection B and C respectively.

### A. The Characteristic Analysis of Upsampling and Mean Filtering Operation Chains

The probability matrix spectrums are widely leveraged in the detection of upsampling operation, because the linear interpolation process of upsampling will lead to periodic characteristics of the p-map [7]. In order to detect upsampling operation, we calculate the p-map for each type of image based on Popescus expectation maximization algorithm [3] and use Fourier changes to observe the image features of different operating chains.

Take Fig. 1(a) as an example. Fig. 1(b) -1(e) shows the different fingerprints in the DFT of the p-map under each hypothesis. If only upsampling is applied on the image, a periodic peak can be found in the corresponding spectrum which appears in the form of symmetrical bright spots. We examine

the p-map and its DFT of a mean filtered image, and discover a periodic fluctuation of energy in the corresponding spectrum. Besides, energy is regionalized and exhibits symmetry and regular changes. As for Fig. 1(e), given that the mean filter is conducted as a post-operation, the fingerprints of upsampling are weakened. In the meantime, the fingerprints of the mean filtering are impaired by upsampling. It is manifested by the enhancement of the noise energy around the low-frequency region and the slight periodic fluctuation of energy. As shown in Fig. 1(f), the cyclical fluctuations in energy are too weak to observe.

Based on unique fingerprints found in the DFT of the p-map of each hypothesis, we design two features to distinguish these hypotheses. One is to detect the existence of four peaks and measure the intensity of these peaks. The other is to capture diagonal noise energy curves.

### B. Symmetry-based PSNR

Symmetry-based PSNR which measures the intensity of the peak relative to the nearby noise is one of the features. We first extract the center horizontal line of the assumed DFT of the p-map and plot the amplitude of each pixel on these lines to select the appropriate threshold. Due to the symmetry of the DFT of the p-map, we directly calculate the PSNR by a half of the pixels from the center horizontal line.

In ref. [20], Chu et al. designed the peak signal-to-noise ratio feature which is used to measure the strength of the peaks with respect to noises nearby. However, the method of extracting PSNR does not consider the symmetry of DFTs of images p-maps. It is shown that the application of symmetry simplifies the PSNR calculation. We first linearize the left half of the center horizontal line to make the noise mean consistent and the peak more prominent. After estimating the parameters of the linear regression using the least square method, we are able to obtain the difference signal  $d_l$ . It can be observed that the DFT of the p-map is symmetric, so PSNR of the entire center horizontal line can be computed directly by the  $PSNR_h$ . We take advantage of the symmetry to calculate the  $PSNR_h$  as follows

$$PSNR_h = \frac{y_p}{ave_{0 < |x - x_p| < \varepsilon}(|d_l(x)|)} \quad (1)$$

Where  $(x_p, y_p)$  and  $\varepsilon$  denote the coordinate of the maximum in  $d_l$  and a small positive constant respectively, and  $ave$  is the approach to calculate average value.

Given that the peak is also present in the center vertical line of the DFTs of images' p-maps, PSNR of the center vertical line signal can be computed with similar procedures, denoted as  $PSNR_v$ . The final value of PSNR is

$$PSNR_s = \max(PSNR_h, PSNR_v) \quad (2)$$

### C. The Fourth Order Energy Fitting Curve

To further distinguish among the hypotheses, we examine fingerprints of mean filtering. Fig. 1(d) and Fig. 1(f) show that when mean filtering is a post-operation, an increase and periodical fluctuation of the overall energy in DFT of the pmap

can be observed. To be more precise, this energy change is enhanced by mean filtering.

Through calculating a summation of neighboring magnitudes in the DFT of an image's p-map, we get the enhanced DFT of the p-map and extract a half of diagonal energy from it. As shown in Fig. 2, the dotted blue lines are noise energy pattern signals. These signals are used for curve fitting to obtain simulated curves within an appropriate range.

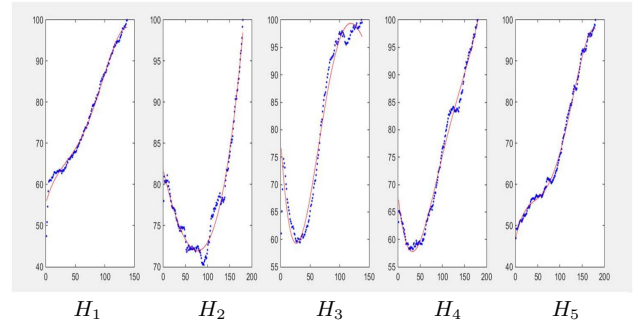


Fig. 2. The noise energy pattern signal (dotted blue lines) extracted from a half of the p-map and their polynomial fitting curves (solid red lines).

Compare the fitting process of various functions, they have different degrees of fitting effect to operation chains. While in terms of the overall fitting effect for five situations, it is found that the fourth order simulation curve fits the noise energy pattern signals better than other types of estimated curves. The solid red lines in Fig. 2 are the estimated curves. The fitted energy curve  $y_n$  is as follows,

$$y_n = ax^4 + bx^3 + cx^2 + dx + e \quad (3)$$

Where  $y_n$  denotes the fitted curve.

Despite the fourth order fitting curve fits well, there is a certain deviation between the fitted curve and the actual curve. Thus, this feature cannot be completely described by the fitted curve. We utilize the variance of the noise energy pattern signals to present the error and the fluctuations between the fitted and the actual curves.

$$d_i = \sum_{m=1}^k (x_m - y_m)^2 / k \quad (4)$$

Where  $x_m$  and  $y_m$  denote actual signal and estimated signal respectively, and  $k$  defines the number of the noise energy pattern signals.

Combining these values together, we take advantage of the coefficient  $a, b, c, d, e$  of the fitted curve  $y_n$  and the variance  $d_i$  to measure the energy curve. Then, by examining the estimated signal, we can detect whether the overall energy increases and fluctuates periodically.

### III. THE IMPACTS OF OPERATING INTENSITY CHANGES

In this section, we analyze fingerprints in DFTs of p-maps of images which with different strengths of upsampling and mean filtering. The aim of analyses is to observe scenarios

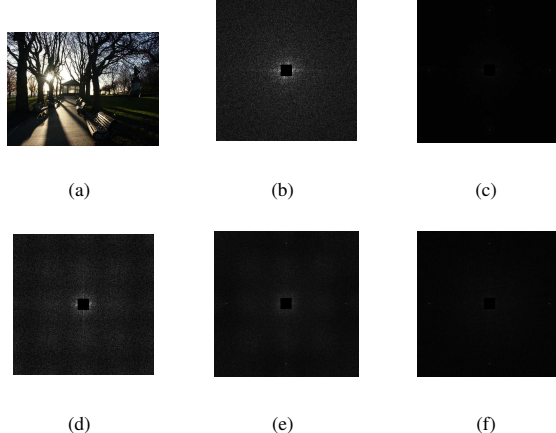


Fig. 3.

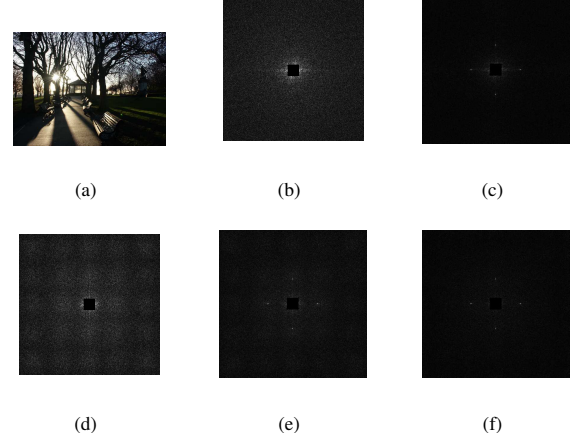


Fig. 4.

For Fig. 3 and Fig. 4, (a) is the original image. (b) - (f) show the DFTs of p-map of images. The operations of images are same as (b) - (f) in Fig. 1. Fig. 3 presents a specific example that the zoom factor is 1.7 and the filter window size is 4, while another example that the zoom factor is 1.2 and the filter window size is 5 shown in Fig. 4.

where these features are ineffective to discriminate the order of operation chains.

#### A. Impacts of Upsampling Operation Intensity Changes

In  $H_4$  and  $H_5$ , if the strength of upsampling continues to increase, the fingerprints of mean filter operation will be too weak to be detected sometime. Eventually, the fingerprints of them become similar as in  $H_2$ . It results in the ineffectiveness of features and the undetectability of operation chains.

As shown in Fig. 3, when the scaling factor increases from 1.3 to 1.7 and the other parameters remain unchanged, Fig. 3(c,e,f) are similar, which causes the failure of distinguishing the operation chains. The bright spot fingerprints of upsampling operation still exist in Fig. 3(c,e,f). Fig. 3 can be inferred that upsampling may affect the fingerprints of mean filtering when intensities of upsampling enhance. In a typical case where the strength of upsampling becomes strong enough, the fingerprints of upsampling, upsampling then mean filtering and mean filtering then upsampling are the same. As a result, the order of operations cannot be detected.

#### B. Impacts of Mean Filtering Operation Intensity Changes

If mean filtering is applied as the last operation and its intensity continues to increase, fingerprints of upsampling will be covered eventually so that they become similar as the DFT of the p-map of  $H_3$ . Thus, the order of operation chains becomes undetectable. In the case where filtering window increases from 4 to 7 and the other factors remain unchanged, the DFTs of p-maps of  $H_3$  and  $H_4$  are alike leading to the undetectability of the operation order. The bright spots which are fingerprints of upsampling operation still can be observed in DFTs of  $H_2$  and  $H_5$ . At the same time, according to the enhanced probability spectra, the noise energy of  $H_2$  and  $H_5$  are different.  $H_5$  keeps its detectability when mean filter

intensity changes. In this case, we are merely able to detect operation chains of  $H_2$  and  $H_5$  by the proposed features.

#### C. Impacts of Multiple Operating Intensity Changes

The next case study we examine is the situation when both intensities of upsampling and mean filtering change. It can be observed that their fingerprints may not be altered, which means five hypotheses can also be distinguished by the proposed two features.

Compared with Fig. 1, the scaling factor reduces from 1.3 to 1.2, and the filtering window increases from 4 to 5. These five hypotheses in Fig. 4 still have their unique fingerprints. Moreover, these fingerprints are similar to those in Fig. 1. Namely, we can extract the features depending on these fingerprints to detect the operation chain. It is worth noting that some operation chains with different strengths have similar fingerprints in each hypothesis and the features are still effective. So the orders of these operation chains can be successfully distinguished.

## IV. EXPERIMENTAL RESULTS

In this section, several experimental results are given to demonstrate the effectiveness of our proposed method for detecting the order of operations.

#### A. Experiment Setting

Since there are five possibilities of the operation order, we set the following five categories of images.

- (1)  $ori$  denotes original images;
- (2)  $us$  denotes upsampled images;
- (3)  $mf$  denotes mean filtered images;
- (4)  $usmf$  denotes upsampled and then mean filtered images;
- (5)  $mfus$  denotes mean filtered and then upsampled images.

To verify the effectiveness of the designed method, we performed a test by including in the dataset 1338 uncompressed

images with the size of  $384 \times 512$  or  $512 \times 384$  in TIFF format from the UCID database [22]. Then we process 1338 unaltered images using different settings for the scaling factor, filtering window size and the cross matching between scaling factor and filtering window size, as reported in Table I.

TABLE I  
OPERATIONS ARE USED TO CREATE THE IMAGE DATASET

Operations	Descriptions
<i>null</i>	The images are not altered by any operations
<i>us</i>	Upsampled, where scaling factor $s = 1.3, 1.4, 1.5, 1.6, 1.7$
<i>mf</i>	Mean filtered, where filter window size $\gamma = 4, 5, 6$
<i>usmf</i>	Upsampled and then mean filtered, $s = 1.3, 1.4, 1.5, 1.6, 1.7; \gamma = 4, 5, 6$
<i>mfus</i>	Mean filtered and then upsampled, $\gamma = 4, 5, 6; s = 1.3, 1.4, 1.5, 1.6, 1.7$ .

Since we consider 5 scaling factors and 3 filtering window sizes, the constructed image dataset contains  $1338+1338 \times 5 + 1338 \times 3 + 1338 \times 5 \times 3 + 1338 \times 3 \times 5 = 52182$  images. Then, this dataset is split in halves to generate the SVM training and test sets. It is worth mentioning that each version of a given original image is always set up in the similar quantity, so as to avoid biases in the training stages. Images copy themselves several times, resulting in  $5 \times 1338$  unaltered images and  $7.5 \times 1338$  altered images of each other category for the training set. Next, the set of forensic features is extracted for each image, and the SVM is trained with those images in the training test. In this experiment, the LIBSVM with a radial basis function(RBF) kernel is adopted.

### B. Order Detecting of Single Parameter

Following the parameters settings in the subsection A, we can firstly obtain detecting accuracies of the cases where only one of upsampling and mean filtering's strength changes. Table II and Table III present detection rates of each category under different scaling factors and filter window sizes, respectively.

TABLE II  
DETECTING ACCURACY OF EACH SCALING FACTOR

Scaling factor size	<i>ori</i>	<i>us</i>	<i>mf</i>	<i>usmf</i>	<i>mfus</i>
1.3	0.91	0.99	0.73	0.92	0.89
1.4	0.91	0.97	0.73	0.91	0.96
1.5	0.91	0.93	0.73	0.91	0.91
1.6	0.91	0.95	0.73	0.90	0.99
1.7	0.91	0.96	0.73	0.92	0.99

As shown in Table II and Table III, the method achieves a good performance. The detection rate of each scaling factor in

TABLE III  
DETECTING ACCURACY OF EACH FILTER WINDOW SIZE

Filter window size	<i>ori</i>	<i>us</i>	<i>mf</i>	<i>usmf</i>	<i>mfus</i>
4	0.91	0.96	0.82	0.91	0.88
5	0.91	0.96	0.81	0.88	0.97
6	0.91	0.96	0.56	0.95	0.99

Table II is similar, meaning the change of scaling factors does not play a significant role in detecting accuracies. It can be observed from Table III that the filtering window size is the main factor influencing detection rates, especially indicating the detection correctnesses of *mf* decrease with the increasing filtering window size.

Overall, the detecting rates of *mf* are obviously lower than other hypotheses. The case examined in the previous section III-B is available to illustrate which hypotheses are confused to make it indistinguishable. When the strength of mean filtering operation continues to enhance in *usmf*, the effect of later applied mean filtering on the fingerprints of previously applied upsampling is more obvious. As the intensity reaches a certain point, its fingerprints become similar as *mf*, leading to the low accuracy of *mf*. It is worth investigating other function forms for detecting image precisely, such as new features and approaches. That is a part of our future work.

### C. Order Detecting of Mixed Parameters

To further verify our proposed method has the universal applicability of detecting images with various strengths, we consider the case where 39 classes must be discriminated by the SVM classifier, corresponding to each scaling factor, each filtering window size or each possible pair of the 5 scaling factors and the 3 filter window sizes in the dataset. The detection accuracy of each type shown in Table IV demonstrates the effectiveness of this proposed method on detecting the image library.

TABLE IV  
CONFUSION MATRIX OF THE IMAGE LIBRARY

Predicted Actual \ \	<i>ori</i>	<i>us</i>	<i>mf</i>	<i>usmf</i>	<i>mfus</i>
<i>ori</i>	0.91	0	0.01	0.09	0
<i>us</i>	0	0.96	0	0.02	0.02
<i>mf</i>	0.01	0	0.73	0.26	0
<i>usmf</i>	0.02	0.02	0.04	0.91	0.01
<i>mfus</i>	0	0.03	0	0.02	0.95

As expected, most categories get good detecting accuracies, while *uf* is not detected successfully. Similar as the Table II and Table III, *mf* presents the low detectable rate. According to the figure for *mf*, this indicates that the confusing hypotheses which make the order undetectable are *mf* and *usmf*. This matches the results shown in the section III-B

where the fingerprints of mean filtering and upsampling then mean filtering are similar and can be hardly distinguished. In addition, the reason of why these two hypotheses are confused is summarized as the enhancement of the intensity of mean filtering operation which effects the fingerprints of upsampling. The undetectability of mf contains typical indistinguishable cases for different pairs of the scale factor and filtering window.

We have to remark that since there are no previous works in the literature addressing the problem of upsampling and mean filtering, we cannot compare the performance of our schemes with other approaches.

## V. CONCLUSION

In this paper, we present a method to detect the order of upsampling and mean filtering operations. The main contributions of the paper are as follows:

- Different from existing techniques, the proposed method focuses on detecting the order of two operations which have not been considered before, namely upsampling and mean filtering.
- Significant features are extracted to detect the order of operation chains including symmetry-based PSNR, the fourth order energy fitting curve as well as the variance of the fitting curve. To verify that the two features can be utilized widely in detecting operation chains, we analyze whether the fingerprints will change in DFTs of images with different intensities of operating.
- In order to test the designed method is able to detect images with different intensities together, we apply our proposed method to various images with mixed strengths. And experimental results demonstrate that the method is very promising for universal use in such a forensic problem.

We would like to point out, the presented work merely could be regarded as an off-the-shelf detection technique that distinguishes the order of upsampling and mean filtering in uncompressed images, but the application of this detector on compressed images still needs to be examined in the future research.

## ACKNOWLEDGMENT

This work is supported by National Natural Science Foundation of China (Grant Nos. 61402162, 61772191, 61472131, 61472129), Hunan Provincial Natural Science Foundation of China (Grant No. 2017JJ3040), Open Research Fund of Key Laboratory of Network Crime Investigation of Hunan Provincial Colleges (Grant No. 2017WLFZZC001), Applied Sci-Tech R&D Special Fund Program of Guangdong Province (Grant No. 2015B010131007), Science and Technology Planning Project of Guangdong Province, China (Grant No. 2017B050506002), the National Key Research and Development Program of China (Grant No. 2018YFB07040), Science and Technology Key Projects of Hunan Province (Grant Nos. 2015TP1004, 2016JC2012).

## REFERENCES

- [1] Bianchi T and Piva A, "Engineering of double JPEG compression in the presence of image resizing," in *Proc. IEEE Int. Workshop on Information Forensics and Security*, Tenerife, Spain, pp. 127-132, 2012.
- [2] Stamm M C, Wu M, and Liu K J R, "Information forensics: An overview of the first decade," *IEEE Access*, vol. 1, pp. 167-200, 2013.
- [3] Popescu A C and Farid H, "Exposing digital forgeries by detecting traces of resampling," *IEEE Trans. Signal Processing*, vol. 53, no. 2, pp. 758-767, 2005.
- [4] O'Brien J F and Farid H, "Exposing photo manipulation with inconsistent reflections," *Acm Trans. Graphics*, vol. 31, no. 1, pp. 1-11, 2012.
- [5] Fridrich J, Soukal D and Lukáš J, "Detection of copy-move forgery in digital images," in *Proc. Digital Forensic Research Workshop*, Cleveland, USA, pp. 1-10, 2003.
- [6] Ng T T and Chang S F, "A model for image splicing," in *Proc. IEEE Int. Conf. Image Processing*, Singapore City, Singapore, pp. 1169-1172, 2004.
- [7] Zhao X, Wang S, Li S and Li J, "Passive image-splicing detection by a 2-D noncausal Markov model," *IEEE Trans. Circuits and Systems for Video Technology*, vol. 25, no. 2, pp. 185-199, 2015.
- [8] Popescu A C and Farid H, "Statistical tools for digital forensics," in *Proc. Int. Workshop on Information Information Hiding*, Toronto, Canada, pp. 128-147, 2004.
- [9] Pevny T and Fridrich J, "Detection of double-compression in JPEG images for applications in steganography," *IEEE Trans. Information Forensics and Security*, vol. 3, no. 2, pp. 247-258, 2008.
- [10] Li W, Yuan Y, and Yu N, "Passive detection of doctored JPEG image via block artifact grid extraction," *Signal Processing*, vol. 89, no. 9, pp. 1821-1829, 2009.
- [11] Kirchner M and Fridrich J, "On detection of median filtering in digital images," *SPIE Electronic Imaging Symposium: Media Forensics and Security II*, San Jose, CA, USA, pp. 1-12, 2010.
- [12] Cao G, Zhao Y, Ni R, Yu L and Tian H, "Forensic detection of median filtering in digital images," in *Proc. IEEE Int. Conf. Multimedia and Expo.*, Suntec City, Singapore, pp. 89-94, 2010.
- [13] Stamm M C and Liu K J R, "Forensic detection of image manipulation using statistical intrinsic fingerprints," *IEEE Trans. Information Forensics and Security*, vol. 5, no. 3, pp. 492-506, 2010.
- [14] Singh N, Gupta A and Jain R C, "Global contrast enhancement based image forensics using statistical features," *Advances in Electrical and Electronic Engineering*, vol. 15, no. 3, pp. 509-516, 2017.
- [15] Zhang Q, Wang H and Hu J, "Blurring Detection in Image Forensics Based on the Posterior Probability," in *Proc. IEEE Int. Conf. System Science, Engineering Design and Manufacturing Informatization*, Chengdu, China, pp. 162-165, 2012.
- [16] Yang B and Liu B, "Feature Fusion for Blurring Detection in Image Forensics," *IEICE Trans. on Information and Systems*, vol. 97, no. 6, pp. 1690-1693, 2014.
- [17] Chen Z, Zhao Y and Ni R, "Detection of Operation Chain: JPEG-Resampling-JPEG," *Signal Processing: Image Communication*, vol. 57, pp. 8-20, 2017.
- [18] Gao S, Liao X, Guo S, Li X and Vijayakumar P, "Forensic Detection for Image Operation Order: Resizing and Contrast Enhancement," in *Proc. Int. Conf. Security, Privacy and Anonymity in Computation, Communication and Storage*, Guangzhou, China, pp. 570-580, 2017.
- [19] Stamm M C, Chu X and Liu K J R, "Forensically determining the order of signal processing operations," in *Proc. IEEE Int. Workshop on Information Forensics and Security*, Guangzhou, China, pp. 162-167, 2013.
- [20] Chu X, Chen Y and Liu K J R, "Detectability of the Order of Operations: An Information Theoretic Approach," *IEEE Trans. Information Forensics and Security*, vol. 11, no. 4, pp. 823-836, 2015.
- [21] Vázquez-Padín D, Comesáñ P and Pérez-González F, "An SVD approach to forensic image resampling detection," in *Proc. European Signal Processing Conference*, Nice, French, pp. 2067-2071, 2015.
- [22] Schaefer G and Stich M, "UCID-An uncompressed colour image database," in *Proc. SPIE, Storage and Retrieval Methods and Applications for Multimedia*, San Jose, USA, pp. 472-480, 2004.